I&EC research
Industrial & Engineering Chemistry Research

Article

pubs.acs.org/IECR

Preparation of Activated Carbon-SnO_2, TiO_2, and WO_3 Catalysts. Study by FT-IR Spectroscopy

Adrián Barroso-Bogeat,[†] María Alexandre-Franco,[†] Carmen Fernández-González,[†] Antonio Macías-García,[‡] and Vicente Gómez-Serrano*[,†]

[†]Department of Organic and Inorganic Chemistry, Faculty of Sciences and [‡]Department of Mechanical Engineering, Energetic and of Materials, School of Industrial Engineering, University of Extremadura, 06006 Badajoz, Spain

ABSTRACT: The chemical changes produced in the surface of activated carbon as a result of the process of preparation of activated carbon−metal oxide catalysts from $SnCl_2$, TiO_2, and Na_2WO_4 in water at pH 1.37 for $SnCl_2$, 5.84 for TiO_2, and 9.54 for Na_2WO_4 are studied. The samples were first prepared by the wet impregnation method in two successive steps of soaking at 80 °C for 5 h and oven-drying at 120 °C for 24 h. Then, they were analyzed by elemental analysis, FT-IR spectroscopy, and measurement of pH of the point of zero charge (pH_{pzc}). The process yield was 149 wt % with $SnCl_2$, 103 wt % with TiO_2, and 106 wt % with Na_2WO_4. The impregnation of the carbon with the catalyst precursors in water entails the oxidation of chromene and pyrone type structures with formation of carboxylic acid groups. pH_{pzc} is 10.50, activated carbon; <1.60, $SnCl_2$; 9.35, TiO_2; and 7.90, Na_2WO_4. The changes originating in the surface chemistry of AC with influence on the acid−base character are stronger by the order $SnCl_2 \gg Na_2WO_4 > TiO_2$.

INTRODUCTION

In heterogeneous catalysis, activated carbon (AC) is used as a catalyst and mainly as a support for catalysts. As a support, high-surface-area microporous ACs are the most commonly used materials as very high catalyst dispersions can be achieved easily, thus resulting in high catalytic activity.[1,2] An additional virtue of ACs is the combined effect of molecular sieving, similar to that of zeolite.[1] Furthermore, they are resistant to acidic and basic media.[3] However, it has also been stated that carbon as a support material is much less inert than assumed by the catalysis community.[1] In many cases, the role of the carbon support is not restricted to providing a large surface on which the sintering of the active catalytic species will be minimized. In the catalyst preparation the interaction between the liquid catalyst precursor and the carbon surface is crucial and often misunderstood.[1] That is why new insights into the chemical changes produced on AC's surface because of the process of preparation of the catalyst support are needed with a view to tailoring the catalyst composition to benefit its activity in catalysis processes and also for regeneration purposes. Metal oxide (MO) catalysts such as SnO_2, TiO_2, and WO_3 supported on AC have been used for a great variety of chemical reactions.[4] In recent years, AC/TiO_2 photocatalysts in particular have drawn vast interest due to their potential to degrade organic micropollutants in water.[5−20] Herein, the chemical changes produced in the surface of AC and in its acid−base character as a result of the preparation of the AC-MO samples from $SnCl_2$, TiO_2, and WO_4^{2-} in water by the wet impregnation method are studied by means of FT-IR spectroscopy and also by measuring pH of the point of zero charge. Data of the elemental composition for the samples are also reported.

MATERIALS AND METHODS

Materials and Reagents. In the preparation of the AC-MO samples, a granular AC (Merck; Darmstadt, Germany, Cod. 1.02514.1000;1.5 mm average particle size) and $SnCl_2 \cdot 2H_2O$ and $Na_2WO_4 \cdot 2H_2O$ (Panreac; Barcelona, Spain; reagent grade) and anatase powder (Aldrich; Steinheim, Germany; particle size lower than 44 μm) were used. The starting AC was previously studied from the standpoint of surface functional groups and structures.[21] Also, the AC-MO samples were characterized in terms of porous structure and chemical composition.[22,23] The impregnation solutions were prepared from deionized water at pH 5.05. The pH of the impregnation solutions is listed in Table 1. Such solutions were used immediately after preparation, without previous deaeration.

Table 1. Preparation of the Samples

precursor	pH	yield (wt %)	codes
$SnCl_2 \cdot 2H_2O$	1.37	149	S120
TiO_2 anatase	5.84	103	T120
$Na_2WO_4 \cdot 2H_2O$	9.54	106	W120

Preparation of the Samples. The preparation of the AC-MO samples was carried out by the wet impregnation method in two successive steps of soaking at 80 °C for 5 h and oven-drying at 120 °C for 24 h, as described in detail elsewhere.[22,23] In the case of TiO_2, however, a slightly modified impregnation method at high temperature previously proposed by Kahn and Mazyck was used.[24,25] In such a method, 25 g of AC was impregnated with 250 mL of an aqueous suspension containing 1.25 g of anatase powder, and the resulting mixture was also

Special Issue: International Conference on Chemical and Biochemical Engineering 2015

Received: November 30, 2015
Revised: January 25, 2016
Accepted: February 1, 2016
Published: February 1, 2016

DOI: 10.1021/acs.iecr.5b04563
Ind. Eng. Chem. Res. 2016, 55, 5200−5206

heated at 80 °C for 5 h under stirring of 300 rpm. After vacuum-filtration, the resulting solid in two successive steps was thoroughly washed with deionized water until total color loss in the residual liquid and oven-dried at 120 °C for 24 h. Anatase was selected as the catalyst precursor because the photocatalytic activity of TiO_2 seems to be mainly associated with the anatase-type structure.[26] The yield of the process of preparation of the samples was estimated by the following expression

$$Y\ (\text{wt}\ \%) = \frac{M_f(g)}{M_i(g)} \cdot 100 \quad (1)$$

where M_i is the initial mass of AC, and M_f is the final mass of AC-MO sample. The yield values are given in Table 1, together with sample codes.

Analysis of the Samples. The elemental analysis of the samples (C, H, N, and S) was performed in an analyzer (CHNS-932, LECO), whereas the O content was estimated by difference. In addition, the samples were analyzed by FT-IR spectroscopy, using a PerkinElmer Spectrum 100 spectrometer. Spectra were recorded in the range of wave numbers from 4000 to 400 cm^{-1}, using sample/KBr pellets prepared as described elsewhere.[21] pH of the point of zero charge (pH_{pzc}) was determined following the method previously proposed by Newcombe et al.[27,28] 0.01 M NaCl aqueous solutions at pH 2, 4, 6, 8, and 10 were prepared by fixing these pH values with either 0.1 M HCl or NaOH aqueous solution. The pH_{pzc} was obtained from the plot of pH of the initial solution against pH of the corresponding supernatant.

RESULTS AND DISCUSSION

Solution/Suspension pH. The pH of the impregnation solution (see Table 1) was 1.37 for $SnCl_2$, 5.84 for TiO_2, and 9.54 for WO_4^{2-}. As regard $SnCl_2$, the freshly prepared aqueous solution looked cloudy with a milk-white appearance. From the low pH of the $SnCl_2$ solution it becomes clear that in the preparation of this solution chemical changes occurred in $SnCl_2$ after contact with water. Stannous chloride is readily soluble in water, its solubility being as high as 178 g of $SnCl_2$ per 100 g of water at 10 °C.[29] The chemical behavior of $SnCl_2$ in excess water depends on a number of factors including solution pH, concentration, storage time, and presence of aerial oxygen.[30−35] Among other processes, $SnCl_2$ undergoes hydrolysis and oxidation with formation of HCl which accounts for the great pH decrease for the $SnCl_2$ solution. Titanium dioxide in water must be hydroxylated. In fact, the TiO_2 surface is known to be readily covered with hydroxyl groups in a water-rich environment,[36] as TiO_2 has both Lewis acidic and basic centers which allow its surface to be easily hydroxylated by dissociative and molecular water adsorption.[37] The pH of 9.54 for the $Na_2WO_4 \cdot 2H_2O$ solution falls within the pH range 9.15−10.5 reported in the literature for molar solutions prepared from $Na_2WO_4 \cdot 2H_2O$ and purified water.[38] The alkalinity of the WO_4^{2-} solution may be due to the presence of excess alkali (i.e., NaOH) in commercial $Na_2WO_4 \cdot 2H_2O$ or to the hydrolysis and polymerization of Na_2WO_4.[38]

Process Yield. As shown in Table 1, the yield of the process of preparation of the samples was 149 wt % for S120, 103 wt % for T120, and 106 wt % for W120 and therefore strongly dependent on the nature of the chemical species used in the impregnation of AC. Probably, a major factor influencing the process yield was the existing speciation in the impregnation solution as it should control mass transport in pores of the carbon and thereby the amount of catalyst precursor ultimately loaded on AC. First, the very high yield for S120 is compatible with a facilitated diffusion of small size tin species in the accessible porosity of AC. Perhaps, as the impregnation of AC with the aforesaid $SnCl_2$ solution was carried out immediately after preparation, large tin polynuclear and polymerized species were formed only to a reduced extent. Likewise, the proportion and size of colloidal particles should be small in the freshly prepared $SnCl_2$ solution. In fact, as reported elsewhere,[33] colloids are composed of tin species such as SnO_2 and Sn_3O_4. Furthermore, SnO_2 originates as soon as $SnCl_2$ is brought into contact with air.[39] Second, the lower yield for T120 can be accounted for by the large size of the TiO_2 (anatase) particles which could not enter a very important fraction of the AC porosity as AC is mainly a microporous carbon.[22] Third, the much lower yield for W120 than for S120 denotes the involvement of larger size species in the diffusion process for the sample prepared with WO_4^{2-}. In the presence of AC, the WO_4^{2-} anion should provide the medium with an O^{2-} ion (i.e., pK_{eq} for $O^{2-} + H_2O = 2OH^-$ being ∼−22), and this leads to the formation of WO_3.

Elemental Composition. Data of the elemental analysis (C, H, N, and S; O, by difference) obtained for AC, S120, T120, and W120 are listed in Table 2. As expected, they show

Table 2. Elemental Analysis of AC and AC-MO Samples

sample	C (wt %)	H (wt %)	N (wt %)	S (wt %)	$O_{diff.}$ (wt %)
AC	86.50	0.51	0.26	0.64	12.09
S120	52.32	1.25	0.06	0.37	46.00
T120	85.81	0.20	0.55	0.63	12.81
W120	78.32	0.98	0.20	0.61	19.89

that carbon is the predominant element in AC. Oxygen is also an abundant chemical constituent of AC, although much less than for carbon. However, hydrogen, nitrogen, and sulfur are minor heteroatoms in AC. As compared to AC, the C, N, and S contents are more or less lower for S120 and W120, in accordance with the process yield. Conversely, the O and H contents are much higher for S120 and W120, which is in line with the incorporation of oxygen as SnO_2 and WO_3 to AC and also with the trend exhibited by these metal oxides to hydration, as demonstrated by the presence of two water molecules in the compounds used in the preparation of the impregnation solutions in the present study. In marked contrast especially to S120, the C and O contents are similar for T120 and AC. However, the H content is much lower for T120 than for AC, and the N content is much higher for T120. From these results it becomes apparent that during the preparation of T120 the incorporation of O as TiO_2 to AC was accompanied by the removal of not only O but also of H, maybe as H_2O.

Infrared Analysis. The FT-IR spectra registered for S120, T120, and W120 are shown in Figures 1 and 2, together with the spectrum of AC which has also been plotted together with the spectra for the AC-MO samples for comparison purposes. Between 4000 and 2000 cm^{-1} all spectra have been plotted on an expanded *y*-axis scale in order to make easier their analysis. The number of features shown in the spectrum of AC were tentatively ascribed elsewhere and summarized in Table 3.[21]

Sample S120. With respect to the spectrum of AC, in the spectrum of S120 (Figures 1 and 2) a series of major changes concerning the number, position, and intensity of registered bands are noted in the analyzed spectral regions of 4000−2000

DOI: 10.1021/acs.iecr.5b04563
Ind. Eng. Chem. Res. 2016, 55, 5200−5206

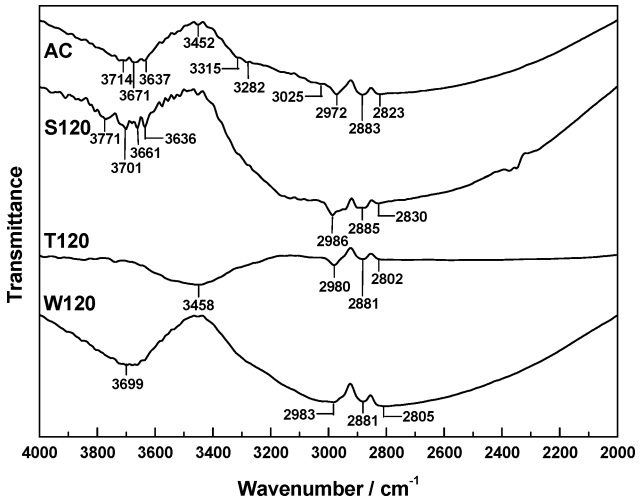

Figure 1. FT-IR spectra of AC, S120, T120, and W120 between 4000 and 2000 cm^{-1}.

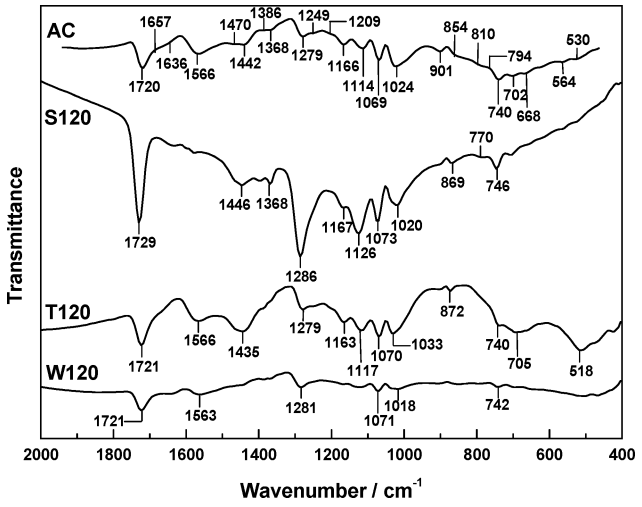

Figure 2. FT-IR spectra of AC, S120, T120, and W120 between 2000 and 400 cm^{-1}.

Table 3. FT-IR Spectrum of AC: Position and Assignment of Bands[a]

spectral feature	position (cm^{-1})	assignment	group/structure
peaks	2972−2823	ν(C−H)	chromene structures
		ν(O−H)	quinone oximes
band	1720	ν(C═O)	carboxylic acid group, 2-pyrone stucture
shoulder	1657	ν(C═O)	pyrone and chromene structures, carbonyl structures
shoulder	1636	ν(C═C)	pyrone and chromene structures
band	1566	ν_s(C═C) skeletal	aromatic ring
		ν(C═C)	2-pyrone structures
band	1279	δ(O−H)−ν(C−O)	carboxylic acid
		ν_{as}(═C−O−C)	4H-chromene
shoulders	ca. 1249	ν_{as}(═C−O−C)	2H-chromene, 2-pyrone
band	1024	ν_s(═C−O−C)	chromene, pyrone, and ether structures

[a]Abbreviations: ν, stretching; δ, bending (in-plane); as, asymmetric; s, symmetric.

and 2000−400 cm^{-1}. First, at frequencies above 3500 cm^{-1}, a new peak appears at 3771 cm^{-1}, and the intensity of the peaks at 3701, 3661, and 3636 cm^{-1} noticeably increases. These features are ascribable to ν(O−H) vibrations of surface hydroxyl groups present in SnO_2. As a general rule, the ν(O−H) absorption frequency depends on the nature of the atom to which the −OH group is bonded and on the coordination of this atom within the surface.[40,41] Therefore, the absorption bands of ν(O−H) vibration appearing in the S120 spectrum argues for surface tin atoms in different coordination states. Second, the shift to higher frequencies and dissimilar shape of the bands at 2986 and 2885 cm^{-1} are also worth mentioning because, according to previous band assignments,[21] these results indicate that chromene structures of AC suffered significant changes because of the process of preparation of S120.

In the spectral region below 2000 cm^{-1} (Figure 2), the great intensity increase of the couple of bands at 1729 and 1286 cm^{-1} is indicative of a greatly enhanced presence of carboxylic acid groups (−COOH) in S120. Characteristic absorptions of the carboxyl group are not only at ∼1700 cm^{-1} (vs) and 1300−1200 cm^{-1} (s) but also at ∼1400 cm^{-1} (m) and ∼900 cm^{-1} (w) due to bond stretching and deformation vibrations.[42] Probably, −COOH groups were generated from pyrone and chromene type structures of AC, as a wide series of spectral features (i.e., shoulders at 1657, 1636, and 1249 cm^{-1}, etc.), which were registered in the spectrum of AC and associated with the aforesaid structures, are not visible in the spectrum of S120. In this connection a very remarkable spectral change concerns the band at 1024 cm^{-1} in the spectrum of AC as this band is shifted to 1020 cm^{-1} and clearly shows a very pronounced absorption decrease (as a guide, see the lower frequency branch from the absorption maximum down to ∼935 cm^{-1}) for S120. In addition, the band at 1020 cm^{-1} is markedly weaker than the band at 1073 cm^{-1} for S120, unlike for AC. Since the band at 1024 cm^{-1} was tentatively ascribed before to the aforementioned reducing structures of AC,[21] the here obtained results corroborate that they were involved in the formation of −COOH groups during the process of preparation of S120. Furthermore, a higher content of −COOH groups in S120 than in AC is also supported by the fact that no readily visible absorption band at around 1560 cm^{-1} is noted in the spectrum of S120, which is compatible with an increased degree of substitution in benzene rings and consequently of symmetry gain and skeletal C═C vibration inactivation. Moreover, the shift of the band from 1720 cm^{-1} for AC to 1729 cm^{-1} for S120 argues for an increase in the content of hydrogen-bonded aliphatic −COOH groups in the case of S120.[43]

A remarkable change in the spectrum of S120 is the markedly broader and stronger band at 1126 cm^{-1} than the bands at 1166 and 1114 cm^{-1} in the spectrum of AC. To an enhanced absorption at around 1126 cm^{-1} may contribute the Sn−OH group and the O_2^-ion because of δ(Sn−OH) and ν(O−O) vibrations. In fact, the corresponding band to the O_2^- ion appears in the frequency range 1180−1060 cm^{-1}.[40] Also, absorption due to the ν(C−O) vibration of C−O−Sn atomic groupings may take place in the spectral region of 1126 cm^{-1}. The medium intensity band lying at 1020 cm^{-1} is attributable to ν_s(C−O−C) vibrations of ether type structures coming from AC,[44] which were chemically stable and remained unaltered after the preparation of S120. The surface Sn−O−Sn linkages absorb below 770 cm^{-1}.[45−48] For crystalline and amorphous components of SnO_2, the band usually appears at 625 and 675

DOI: 10.1021/acs.iecr.5b04563
Ind. Eng. Chem. Res. 2016, 55, 5200−5206

cm^{-1} or at 550 cm^{-1}, respectively.[49] However, in connection with band assignments for SnO_2 it should be taken into account that, as previously reported by Baraton,[50] the performance of infrared studies on SnO_2 surface is handicapped by the instability of the material with regard to stoichiometry. As a consequence of oxygen substoichiometry the conductivity of the material increases, leading to an opacity of the sample to IR radiation.

Likely, the oxidation of surface groups of AC with formation of −COOH groups occurred with involvement of strong oxidizing species generated as a result of the oxidation of Sn(II) (i.e., metastable or dative peroxides which are characterized by a high energy content and great instability)[51] during the soaking step or of O_2 (air) in a reaction catalyzed by SnO_2 during the oven-drying step. As is well-known, many oxides mainly act as a support material for dispersed metal catalysts; tin oxide, however, is an oxidation catalyst in its own right. As in most oxide catalysts the oxidation reactions are supposed to follow the Mars-van Krevelen mechanism. Thus, adsorbed molecules are oxidized by consuming lattice oxygen of the oxide catalyst which in turn is reoxidized by gas-phase oxygen. This is possible because transition and post-transition oxides have multivalent oxidation states that allow the material to easily give up lattice oxygen to react with adsorbed molecules and can be subsequently reoxidized by gas-phase oxygen.[52] As a guide, in the case of SnO_2 its surface exhibits high adsorption properties and high reactivity due to the presence of free electrons in the conduction band and to the presence of surface and volume oxygen vacancies and of active chemisorbed oxygen. Adsorbed oxygen can be present in various chemical species according to the following processes:[53,54]

$$O_2(g) = O_2(ad) = O_2^-(ad) = O^-(ad) = O^{2-}(ad) = O^{2-}(lattice)$$

The temperature dependence of the various species was examined by Chang,[55] observing a transition temperature at 150 °C. Below which oxygen is mainly present as O_2^- and above chemisorbed oxygen in the form of O^- or O^{2-} is present. Depending on the temperature at the surface of transition metal−metal oxides there can appear ions O_2^- or O^- as a result of chemisorption. Ion O_2^- is classified as an "electrophilic" agent, while ion O^{2-} connected with the lattice at the surface behaves as a "nucleophilic" agent.[56,57] Therefore, in the case of our reaction system, oxygen transfer should occur from SnO_2 to AC.

Sample T120. Unlike the spectrum of AC and especially of S120, the spectrum of T120 between 3800 and 3600 cm^{-1} does not show features ascribable to free −OH groups. In the case of T120, the −OH surface groups seem to be involved in hydrogen bonding as the spectrum of this sample displays the broad band centered at 3458 cm^{-1}, which is compatible with the presence of such a physical bond in the sample. Furthermore, phenolic −OH groups were detected in AC, and TiO_2 has a high tendency to hydroxylation,[36,58] as commented above. At lower frequencies in the T120 spectrum, the weak bands at 2980 and 2881 cm^{-1} also appear in the spectrum of AC. Notice that band positions and intensities are similar in the spectra of both samples. Therefore, according to the here obtained FT-IR results, the $-CH_2-$ groups present initially in AC did not undergo appreciable chemical changes after the preparation of T120. Although such groups may be found in a different molecular configuration in both samples, as the band is shifted to slightly higher frequencies for T120.

Below 2000 cm^{-1}, the spectrum of T120 at first sight is also fairly well similarly shaped to the spectrum of AC. Thus, the former spectrum displays the broad series of stronger absorption bands at nearly the same frequencies (i.e., 1721, 1566, 1279, 1163, 1117, 1070, 1033, and 740 cm^{-1}) that are registered as well in the spectrum of AC. Also, shoulders in the frequency ranges 1721−1619 cm^{-1} and 1279−1224 cm^{-1} are readily visible in the spectrum of T120. Therefore, the surface groups and structures of AC were largely preserved after the impregnation of AC with the TiO_2 suspension in the preparation of T120, as expected because TiO_2 is a chemically stable substance.[59] However, the number of shoulders between 1721 and 1619 cm^{-1} and band intensities are different in both spectra. Clearly, the band at 1721 cm^{-1} for T120 is somewhat stronger than the band at 1720 cm^{-1} for AC, whereas the band at 1033 cm^{-1} for T120 is noticeably weaker than the band at 1024 cm^{-1} for AC (for comparison purpose, it can be used the band at 1070 and 1069 cm^{-1} that possesses a similar intensity in both spectra). From these results it is evident that C−O−C containing reducing structures of AC in part, at least, were oxidized and transformed into −COOH groups during the process of preparation of T120. Probably, the oxidation of AC was facilitated as a result of the large particle size of TiO_2 (i.e., lower than 44 μm) which would not effectively prevent the oxidizing agent from entering smaller size pores of AC, where most part of the surface area of microporous solids such as AC concentrates, that would remain then available for oxidation during the preparation of T120. Another spectral change noted in the spectrum of T120 concerns the medium intensity band at 1435 cm^{-1}, which is not registered in the spectrum of S120 and that may be associated with carboxylate groups formed between −COOH groups of AC and TiO_2 surfaces.[58] Alternatively, such a spectral feature may be due to ν(COO−) vibrations of CO_2^- and CO_3^{2-} or HCO_3^- formed after chemisorption of carbon species on TiO_2.[60−62] On the other hand, the spectrum of T120 also displays bands and shoulders in the 800−400 cm^{-1} frequency range that are ascribable to ring substitution and ν(Ti−O) vibrations,[63] according to the strong band at 690 cm^{-1} with a pronounced shoulder at 545 cm^{-1} exhibited by the infrared spectrum obtained separately for the starting anatase used in the preparation of T120, which is plotted in Figure 3.

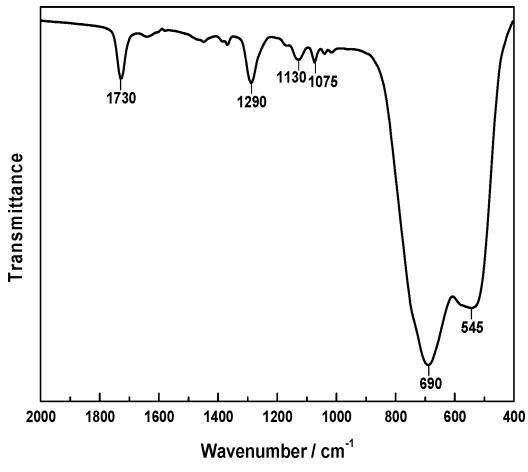

Figure 3. FT-IR spectrum of TiO_2 (anatase powder) between 2000 and 400 cm^{-1}.

DOI: 10.1021/acs.iecr.5b04563
Ind. Eng. Chem. Res. 2016, 55, 5200−5206

Sample W120. The spectrum of W120 between 4000 and 2000 cm^{-1} displays a very broad band in the range 4000−3450 cm^{-1}, which is centered at 3699 cm^{-1} and that is decorated with a large number of barely defined peaks. These spectral features are compatible with the presence in this sample of a variety of free −OH groups, the contents of which being low. Also, molecular water absorbing in such a spectral region may be found in W120 as hydration water of WO_3 that remained in the sample after oven-drying at 120 °C in its preparation. It is supported by the fact that the dehydration of hydrate precursors of both various metastable and stable WO_3 occurs at higher temperatures in the range 235−350 °C.[64] At lower frequencies in the region of 2900−2800 cm^{-1} the only noticeable spectral change is the absence from the spectrum of W120 of the weak peak at 2972 cm^{-1} in the spectrum of AC. Otherwise, there must be overlapping bands on account of the absorption increase produced at higher frequencies. In any event, these results seem to indicate occurrence of changes in the $-CH_2-$ groups of chromene type structures present in AC because of the preparation of W120.

The fact that the spectrum of W120 between 2000 and 400 cm^{-1} only features very weak bands evidence that W120 was little amenable to the infrared analysis, which must be necessarily connected with the presence of WO_3 in this sample. Because tungsten is a very heavy metal, its density being as high as 19.3 g cm^{-3},[65] the content of carbon in the weighed amount of W120 used in the preparation of the W120:KBr pellet was surely low, this affecting the sensitivity of the infrared analysis. Accordingly, a transmittance-axis expanded spectrum was plotted in Figure 4. As compared to the spectrum of AC, it is

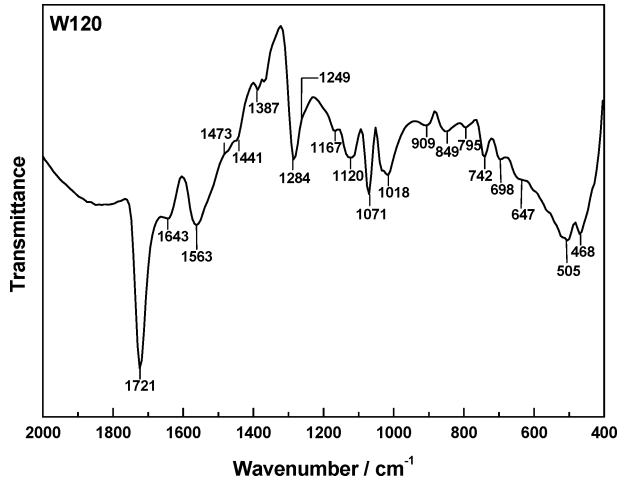

Figure 4. Expanded FT-IR spectrum between 2000 and 400 cm^{-1} for W120.

worth noting the increased intensity of the strong bands at 1721 and 1284 cm^{-1} together with the absence of shoulders at 1657 and 1636 cm^{-1}, which are registered for AC, and the intensity decrease of the band at 1018 cm^{-1}. Therefore, from these results it becomes clear that AC was also oxidized during the preparation of W120 and that reducing structures of AC took part in the oxidation process. Another absorption band registered for W120 is the weak band at 1643 cm^{-1} that is ascribable to OH bending of molecular water present in the sample as hydration water of WO_3. The broad band at 1120 cm^{-1} denotes contribution to absorption of infrared radiation by chemisorbed oxygen and/or C−O−W atomic groupings. At frequencies in the range 1000−600 cm^{-1}, absorption may be caused by ν(W = O) and ν(W−O) vibrations.[66,67] Specifically, the characteristic bond vibration frequency is between 1000 and 948 cm^{-1} for W = O and between 870 and 610 cm^{-1} for W−O, depending on the WO_3 crystalline phase and its degree of hydration.[66]

Comparison of the spectra for S120, T120, and W120 in the regions of around 1720, 1280, and 1120 cm^{-1} suggests that carboxylic acid groups were formed to a larger extent for S120 than for W120 and especially for T120 and that correspondingly the decrease of reducing structures should be also greater for S120. In any event it should be mentioned here that the relative intensity of the bands at around 1070 and 1020 cm^{-1} is rather similar for S120 and W120, unlike for T120. In connection with the reactivity of carbon it was reported before that it is high with oxygen.[68] However, it was also found that carbonaceous materials are not oxidized below 175 °C in air and that the process is slow even when heating at 250 °C.[69] Using AC and $SnCl_2$, TiO_2, and WO_4^{2-} in water, reducing structures of AC are oxidized at lower temperatures, especially when the low-pH $SnCl_2$ solution is used, which is a relevant finding in relation to the changes originated in the surface chemistry of AC as a result of the process of preparation of the AC-MO samples.

pH of the Point of Zero Charge. As shown in Table 4, the pH_{pzc} is 10.50 for AC, <1.60 for S120, 9.35 for T120, and 7.90

Table 4. pH_{pzc} Measured for AC and AC-MO Samples

sample	pH_{pzc}
AC	10.50
S120	<1.60
T120	9.35
W120	7.90

for W120. The high pH_{pzc} for AC is worth noting as it is consistent with the presence of chromene and pyrone type basic structures in the carbon. Evidence for the pyrone-type site as the basic site has been provided before by acid titration and TPD as well as by theoretical calculations.[70−73] Besides the chromene and pyrone types, the basic behavior of carbon surfaces has been associated with the π basicity (or Lewis basicity) of the aromatic rings.[70,74,75] Furthermore, it was stated that the basicity from the aromatic rings is weak, and the main basicity is still attributed to the oxygen containing groups.[76] On the other hand, since chromene and pyrone type structures not only are reducing in character but also basic in character, their removal from AC because of oxidation during the preparation of the samples is reflected by the behavior of the AC-MO samples in acid−base neutralization reactions. Thus, the lower pH_{pzc} for the AC-MO samples than for AC is in line with a basicity decrease and acidity increase produced for the AC-MO samples. From the pH_{pzc} values it becomes apparent that changes originated in surface groups and structures of AC are stronger by the sequence S120 ≫ W120 > T120. For the samples, this sequence is in accord with the extent to which carboxylic acid groups were formed, as shown by the FT-IR analysis of the samples.

CONCLUSIONS

The preparation of AC-MO catalysts by wet impregnation of AC with $SnCl_2$, TiO_2, and WO_4^{2-} in water at pH 1.37, 5.84, and 9.54, which has been carried out into successive soaking and

DOI: 10.1021/acs.iecr.5b04563
Ind. Eng. Chem. Res. 2016, 55, 5200−5206

drying steps, entails marked changes in the surface chemistry of the carbon. By selective oxidation of AC reducing structures, such as chromene and pyrone structures, during the preparation of the samples,−COOH groups to a larger extent especially with SnO_2 than with WO_3 and TiO_2 are formed. pH_{pzc} is 10.50 for AC, <1.60 for S120, 9.35 for T120, and 7.90 for W120, and therefore the AC-MO samples greatly range in the acid−base character of their surface. With respect to AC, the strongest change in such a character occurs for S120. Obtained results are surely of interest for preparative, use in catalysis processes, and regeneration purposes of the AC-MO catalysts.

AUTHOR INFORMATION

Corresponding Author

*E-mail: vgomez@unex.es.

Notes

The authors declare no competing financial interest.

ACKNOWLEDGMENTS

Financial support from Gobierno de Extremadura and Feder funds (GRU07011, GRU09122, and GRU10119) is gratefully acknowledged. A. Barroso-Bogeat thanks Spanish Ministerio de Educación y Cultura for the concession of a FPU grant (AP2010-2574).

REFERENCES

(1) Radovic, L. R; Sudhakar, C. Carbon as a Catalyst Support: Production, Properties and Applications. In *Introduction to Carbon Technologies*; Marsh, H., Heintz, E. A., Rodríguez-Reinoso, F., Eds.; Universidad de Alicante: Alicante, 1997; pp 103−165.

(2) Daza, L.; González Ayuso, T.; Mendioroz, S.; Pajares, J. A. Decomposition of Precursors on Preparation of Rh/Active Carbon Catalysts. *Appl. Catal.* **1985**, *13*, 295.

(3) Rodríguez-Reinoso, F. Activated Carbon: Structure, Characterization, Preparation and Applications. In *Introduction to Carbon Technologies*; Marsh, H., Heintz, E. A., Rodríguez-Reinoso, F., Eds.; Universidad de Alicante: Alicante, 1997; pp 35−101.

(4) Barroso-Bogeat, A.; Fernández-González, C.; Alexandre-Franco, M.; Gómez-Serrano, V. Activated Carbon as a Metal Oxide Support: A Review. In *Activated Carbon: Classifications, Properties and Applications*; Kwiatkowski, J. F., Ed.; Nova Sci. Pub.: New York, 2011; pp 297−318.

(5) Torimoto, T.; Ito, S.; Kuwabata, S.; Yoneyama, H. Effects of Adsorbents used as Supports for Titanium Dioxide Loading on Photocatalytic Degradation of Propyzamide. *Environ. Sci. Technol.* **1996**, *30*, 1275.

(6) Tao, Y.; Schwartz, S.; Wu, C.-Y.; Mazyck, D. W. Development of a TiO_2/AC Composite Photocatalyst by Dry Impregnation for the Treatment of Methanol in Humid Airstreams. *Ind. Eng. Chem. Res.* **2005**, *44*, 7366.

(7) Tao, Y.; Wu, C.-Y.; Mazyck, D. W. Microwave-Assisted Preparation of TiO_2/Activated Carbon Composite Photocatalyst for Removal of Methanol in Humid Air Streams. *Ind. Eng. Chem. Res.* **2006**, *45*, 5110.

(8) Kubo, M.; Fukuda, H.; Chua, X. J.; Yonemoto, T. Kinetics of Ultrasonic Degradation of Phenol in the Presence of Composite Particles of Titanium Dioxide and Activated Carbon. *Ind. Eng. Chem. Res.* **2007**, *46*, 699.

(9) Geng, Q.; Guo, Q.; Cao, C.; Wang, L. Investigation into Nano TiO_2/ACSCR for Decomposition of Aqueous Hydroquinone. *Ind. Eng. Chem. Res.* **2008**, *47*, 2561.

(10) Wang, X.; Liu, Y.; Hu, Z.; Chen, Y.; Liu, W.; Zhao, G. Degradation of Methyl Orange by Composite Photocatalysts nano-TiO_2 Immobilized on Activated Carbons of Different Porosities. *J. Hazard. Mater.* **2009**, *169*, 1061.

(11) Basha, S.; Keane, D.; Morrissey, A.; Nolan, K.; Oelgemöller, M.; Tobin, J. Studies on the Adsorption and Kinetics of Photodegradation of Pharmaceutical Compound, Indomethacin Using Novel Photocatalytic Adsorbents (IPCAs). *Ind. Eng. Chem. Res.* **2010**, *49*, 11302.

(12) Geng, Q.; Cui, W. Adsorption and Photocatalytic Degradation of Reactive Brilliant Red K-2BP by TiO_2/AC in Bubbling Fluidized Bed Photocatalytic Reactor. *Ind. Eng. Chem. Res.* **2010**, *49*, 11321.

(13) Jamil, T. S.; Ghaly, M. Y.; Fathy, N. A.; Abd el-halim, T. A.; Österlund, L. Enhancement of TiO_2 Behavior on Photocatalytic Oxidation of MO Dye Using TiO_2/AC under Visible Irradiation and Sunlight Radiation. *Sep. Purif. Technol.* **2012**, *98*, 270.

(14) Gao, B.; Yap, P. S.; Lim, T. M.; Lim, T. T. Adsorption-Photocatalytic Degradation of Acid Red 88 by Supported TiO_2: Effect of Activated Carbon Support and Aqueous Anions. *Chem. Eng. J.* **2011**, *171*, 1098.

(15) Slimen, H.; Houas, A.; Nogier, J. P. Elaboration of Stable Anatase TiO_2 through Activated Carbon Addition with High Photocatalytic Activity under Visible Light. *J. Photochem. Photobiol., A* **2011**, *221*, 13.

(16) Huang, D.; Miyamoto, Y.; Matsumoto, T.; Tojo, T.; Fan, T.; Ding, J.; Guo, Q.; Zhang, D. Preparation and Characterization of High-Surface-Area TiO_2/Activated Carbon by Low-Temperature Impregnation. *Sep. Purif. Technol.* **2011**, *78*, 9.

(17) Asiltürk, M.; Sener, S. TiO_2-Activated Carbon Photocatalysts: Preparation, Characterization and Photocatalytic Activities. *Chem. Eng. J.* **2012**, *180*, 354.

(18) Mahadwad, O. K.; Parikh, P. A.; Jasra, R. V.; Patil, C. Photocatalytic Degradation of Reactive Black-5 Dye Using TiO_2-Impregnated Activated Carbon. *Environ. Technol.* **2012**, *33*, 307.

(19) Jo, W.-K.; Won, Y.; Hwang, I.; Tayade, R. J. Enhanced Photocatalytic Degradation of Aqueous Nitrobenzene Using Graphitic Carbon-TiO_2 Composites. *Ind. Eng. Chem. Res.* **2014**, *53*, 3455.

(20) Sun, J.; Wang, Y.; Sun, R.; Dong, S. Photodegradation of Azo Dye Congo Red from Aqueous Solution by the WO_3-TiO_2/Activated Carbon (AC) Photocatalyst under the UV Radiation. *Mater. Chem. Phys.* **2009**, *115*, 303.

(21) Barroso-Bogeat, A.; Alexandre-Franco, M.; Fernández-González, C.; Gómez-Serrano, V. FT-IR Analysis of Pyrone and Chromene Structures in Activated Carbon. *Energy Fuels* **2014**, *28*, 4096.

(22) Barroso-Bogeat, A.; Alexandre-Franco, M.; Fernández-González, C.; Gómez-Serrano, V. Preparation of Activated Carbon-Metal Oxide Hybrid Catalysts: Textural Characterization. *Fuel Process. Technol.* **2014**, *126*, 95.

(23) Barroso-Bogeat, A.; Alexandre-Franco, M.; Fernández-González, C.; Gómez-Serrano, V. Preparation and Microstructural Characterization of Activated Carbon-Metal Oxide Hybrid Catalysts: New Insights into Reactions Paths. *J. Mater. Sci. Technol.* **2015**, *31*, 806.

(24) Kahn, A. TiO_2 Coated Activated Carbon for Water Recovery. *J. Undergrad. Res.* **2002**, *3*, June.

(25) El-Sheikh, A. H.; Newman, A. P.; Al-Daffaee, H.; Phull, S.; Cresswell, N.; York, S. Deposition of Anatase on the Surface of Activated Carbon. *Surf. Coat. Technol.* **2004**, *187*, 284−292.

(26) Ao, Y.; Xu, J.; Shen, X.; Fu, D.; Yuan, C. Magnetically Separable Composite Photocatalyst with Enhanced Photocatalytic Activity. *J. Hazard. Mater.* **2008**, *160*, 295−300.

(27) Newcombe, G.; Hayes, R.; Drikas, M. Granular Activated Carbon: Importance of Surface Properties in the Adsorption of Naturally Occurring Organics. *Colloids Surf., A* **1993**, *78*, 65.

(28) Lopez-Ramon, M. V.; Stoeckli, F.; Moreno-Castilla, C.; Carrasco-Marín, F. On the Characterization of Acidic and Basic Surface Sites on Carbons by Various Techniques. *Carbon* **1999**, *37*, 1215.

(29) In *CRC Handbook of Chemistry and Physics*; Lide, D. R., Ed.; 2005−2006 86th ed.; Taylor & Francis: Boca Raton, 2005.

(30) Ortiz, A.; Mendoza, M.; Rodríguez Paez, J. E. Naturaleza y Formación de Complejos Intermedios del Sistema Sn_2Cl_2-NH_4OH-H_2O. *Mater. Res.* **2001**, *4*, 265.

(31) Baes, C. F.; Mesmer, R. E. *The Hydrolysis of Cations*; Wiley: New York, 1976.

DOI: 10.1021/acs.iecr.5b04563
Ind. Eng. Chem. Res. 2016, 55, 5200−5206

(32) Cigala, R. M.; Crea, F.; De Stefano, C.; Lando, G.; Milea, D.; Sammartano, S. The Inorganic Speciation of Tin(II) in Aqueous Solution. *Geochim. Cosmochim. Acta* **2012**, *87*, 1.
(33) Reva, O. V.; Vorobeva, T. N. Oxidation, Hydrolysis and Colloid Formation in Storage of $SnCl_2$ Aqueous Solutions. *Russ. J. Appl. Chem.* **2002**, *75*, 700.
(34) Remi, R. *Treatise of Inorganic Chemistry*; Elsevier: Amsterdam, 1956; Vol. *1*.
(35) Séby, F.; Potin-Gautier, M.; Giffaut, E.; Donard, O. F. X. A Critical Review of Thermodynamic Data for Inorganic Tin Species. *Geochim. Cosmochim. Acta* **2001**, *65*, 3041.
(36) Huang, W.-F.; Chen, H.-T.; Lin, M. C. The Adsorption and Reactions of $SiCl\chi$ (χ = 0−4) on Hydroxylated TiO_2 Anatase (101) Surface: A Computational Study on the Functionalization of Titania with $Cl_2Si(O)O$ Adsorbate. *Comput. Theor. Chem.* **2012**, *993*, 45.
(37) Fahmi, A.; Minot, C. A. Theoretical Investigation of Water Adsorption on Titanium Dioxide Surfaces. *Surf. Sci.* **1994**, *304*, 343.
(38) Freedman, M. J. Polymerization of Anions: The Hydrolysis of Sodium Tungstate and Sodium Chromate. *J. Am. Chem. Soc.* **1958**, *80*, 2072.
(39) Przyluski, J.; Kasprzak, M.; Bielinski, J. Investigations of the $SnCl_2$-Sensitizing Solutions for Electroless Plating. *Surf. Coat. Technol.* **1987**, *31*, 203.
(40) Davydov, A. A. *Infrared Spectroscopy of Adsorbed Species on the Surface of Transition Metal Oxides*; Wiley: Chichester, 1984.
(41) Baraton, M.-I.; Merhari, L. Influence of the Particle Size on the Surface Reactivity and Gas Sensing Properties of SnO_2 Nanoparticles. *Mater. Trans.* **2001**, *42*, 1616.
(42) Schevchenko, L. L. Infrared Spectra of Salts and Complexes of Carboxylic Acids and Some of their Derivatives. *Russ. Chem. Rev.* **1963**, *32*, 201.
(43) Pretsch, E.; Bühlmann, P.; Badertscher, M. *Structure Determination of Organic Compounds. Tables of Spectral Data*; Springer-Verlag: Berlin, Heidelberg, 2009.
(44) Kilimov, A. P.; Svechnikova, M. A.; Shevchenko, V. I.; Smirnov, V. V.; Kvasyuk-Mudryi, F. V.; Zotov, S. B. Infrared Spectra of Cyclic Ethers and their Derivatives. *Chem. Heterocycl. Compd.* **1967**, *3*, 467.
(45) Harrison, P. G.; Guest, A. Tin Oxide Surfaces. *J. Chem. Soc., Faraday Trans. 1* **1987**, *83*, 3383.
(46) Amalric-Popescu, D.; Bozon-Verduraz, F. Infrared Studies on SnO_2 and Pd/SnO_2. *Catal. Today* **2001**, *70*, 139.
(47) Aguilar, C. J.; Ochoa, Y. H.; Rodríguez-Páez, J. E. Obtención de Óxido de Estaño en el Sistema $SnCl_2$-H_2O: Mecanismo de Formación de las Partículas. *Rev. Latin Am. Metal. Mater.* **2013**, *33*, 100.
(48) Martos, M.; Morales, J.; Sánchez, L. Mechanochemical Synthesis of $Sn_{1-x}M_xO_2$ Anode Materials for Li-Ion Batteries. *J. Mater. Chem.* **2002**, *12*, 2979.
(49) Jiménez, V. M.; Caballero, A.; Fernandez, A.; Espinós, J. P.; Ocaña, M.; González-Elipe, A. R. Structural Characterization of Partially Amorphous SnO_2 Nanoparticles by Factor Analysis of XAS and FT-IR Spectra. *Solid State Ionics* **1999**, *116*, 117.
(50) Baraton, M.-I. Fourier Transform Infrared Surface Spectrometry of Nano-Sized Particles. In *Handbook of Nanostructured Materials and Nanotechnology*; Nalwa, H. S., Ed.; Academic Press: San Diego, CA, 1999; pp 89−93.
(51) Haring, R. C.; Walton, J. H. The Autoxidation of Stannous Chloride. II A Survey of Certain Factors Affecting this Reaction. *J. Phys. Chem.* **1933**, *37*, 133.
(52) Batzill, M.; Diebold, U. The Surface and Materials Science of Tin Dioxide. Review. *Prog. Surf. Sci.* **2005**, *79*, 47.
(53) Mizokawa, Y.; Nakamura, S. ESR Study of Adsorbed Oxygen on Tin Dioxide. *Oyo Butury* **1977**, *46*, 580.
(54) Batzill, M. Surface Studies of Gas Sensing Materials: SnO_2. *Sensors* **2006**, *6*, 1345.
(55) Chang, S. C. Oxygen Chemisorption on Tin Oxide: Correlation between Electrical Conductivity and EPR Measurements. *J. Vac. Sci. Technol.* **1980**, *17*, 366.
(56) Bielanski, A.; Haber, J. Oxygen in Catalysis on Transition Metal Oxides. *Catal. Rev.: Sci. Eng.* **1979**, *19*, 1.
(57) Teterycz, H.; Klimkiewicz, R.; Laniecki, M. Study of Physico-Chemical Properties of Tin Dioxide Based Gas Sensitive Materials Used in Condensation Reactions of n-Butanol. *Appl. Catal., A* **2004**, *274*, 49.
(58) Tanner, R. E.; Liang, Y.; Altman, E. I. Structure and Chemical Reactivity of Adsorbed Carboxylic Acids on Anatase TiO_2 (001). *Surf. Sci.* **2002**, *506*, 251.
(59) Zhang, M.; Wu, J.; Lu, D. D.; Yang, J. Enhanced Visible Light Photocatalytic Activity of TiO_2 Nanotube Array Films by co-Doping with Tungsten and Nitrogen. *Int. J. Photoenergy* **2013**, *2013*, 1−471674.
(60) Yates, D. J. C. Infrared Studies of the Surface Hydroxyl Groups on Titanium Dioxide, and of the Chemisorption of Carbon Monoxide and Carbon Dioxide. *J. Phys. Chem.* **1961**, *65*, 746.
(61) Mathieu, M. V.; Primet, M.; Pichat, P. Infrared Study of the Surface of Titanium Dioxides. II: Acidic and Basic Properties. *J. Phys. Chem.* **1971**, *75*, 1221.
(62) El-Bahy, Z. M. Adsorption of CO and NO on Ceria- and Pt-Supported TiO_2: In Situ FTIR Study. *Mod. Res. Catal.* **2013**, *2*, 136.
(63) Vasconcelos, D. C. L.; Costa, V. C.; Nunes, E. H. M.; Sabioni, A. C. S.; Gasparon, M.; Vasconcelos, W. L. Infrared Spectroscopy of Titania Sol-Gel Coatings on 316L Stainless Steel. *Mater. Sci. Appl.* **2011**, *2*, 1375.
(64) Purans, J.; Kuzmin, A.; Guéry, C. *In-Situ* x-Ray Absorption Fine Structure and x-Ray Diffraction Studies of Hydrogen Intercalation in Tungsten Oxides. *Proc. SPIE* **1996**, *2968*, 174.
(65) Emsley, J. *The Elements*; Clarendon Press: London, 1989.
(66) Daniel, M. F.; Desbat, B.; Lassegues, J. C.; Gerand, B.; Figlarz, M. Infrared and Raman Study of WO_3 Tungsten Trioxide and $WO_3.xH_2O$ Tungsten Trioxide Hydrates. *J. Solid State Chem.* **1987**, *67*, 235.
(67) Badilescu, S.; Minh-Ha, N.; Bader, G.; Ashrit, P. V.; Girouard, F. E.; Truong, V.-V. Structure and Infrared Spectra of Sol-Gel Derived Tungsten Oxide thin Films. *J. Mol. Struct.* **1993**, *297*, 393.
(68) Bansal, R. C.; Goyal, M. *Activated Carbon Adsorption*; CRC Taylor & Francis: Boca Raton, FL, 2005.
(69) Gómez-Serrano, V.; Piriz-Almeida, F.; Durán-Valle, C. J.; Pastor-Villegas, J. Formation of Oxygen Structures by Air Activation. A Study by FT-IR Spectroscopy. *Carbon* **1999**, *37*, 1517.
(70) Leon y Leon, C. A.; Solar, J. M.; Calemma, V.; Radovic, L. R. Evidence for the Protonation of Basal Plane Sites on Carbon. *Carbon* **1992**, *30*, 797.
(71) Suárez, D.; Menéndez, J. A.; Fuente, E.; Montes-Morán, M. A. Contribution of Pyrone-Type Structures to Carbon-Basicity: An ab Initio Study. *Langmuir* **1999**, *15*, 3897.
(72) Suárez, D.; Menéndez, J. A.; Fuente, E.; Montes-Morán, M. A. Pyrone-Like Structures as Novel Oxygen-Based Organic Superbases. *Angew. Chem., Int. Ed.* **2000**, *39*, 1320.
(73) Boehm, H. P. Surface Oxides on Carbon and their Analysis: A Critical Assessment. *Carbon* **2002**, *40*, 145.
(74) Boehm, H. P.; Voll, M. Basische Oberflächenoxide auf Kohlenstoff-I. Adsorption von Säuren. *Carbon* **1970**, *8*, 227.
(75) Montes-Morán, M. A.; Menéndez, J. A.; Fuente, E.; Suárez, D. Contribution of the Basal Planes to Carbon Basicity: An ab-Initio Study of the H_2O^+-π Interactions in Cluster Models. *J. Phys. Chem. B* **1998**, *102*, 5595.
(76) Yang, R. T. *Adsorbents: Fundamentals and Applications*; Wiley: Hoboken, 2003.

DOI: 10.1021/acs.iecr.5b04563
Ind. Eng. Chem. Res. 2016, 55, 5200−5206